Performance evaluation of pilot-assisted PAPR reduction technique in optical OFDM systems

Ogunkoya, Funmilayo B.; Popoola, Wasiu O.; Shahrabi, Ali; Sinanovic, Sinan

Published in:
IEEE Photonics Technology Letters

DOI:
10.1109/LPT.2015.2407697

Publication date:
2015

Document Version
Author accepted manuscript

Performance Evaluation of Pilot-assisted PAPR Reduction Technique in Optical OFDM Systems

Funmilayo B. Ogunkoya, Wasiu O. Popoola, Ali Shahrabi, and Sinan Sinanović

***Abstract*—The pilot-assisted peak-to-average power ratio (PAPR) reduction technique proposed for optical orthogonal frequency division multiplexing (OFDM) communication systems is evaluated empirically and theoretically in this letter. The PAPR reduction is achieved by rotating the phase of data symbols with P iterations of randomly generated pilot symbol sequence. The results of our hardware implementation and analysis show a close agreement to that of computer simulations. In comparison with basic OFDM where no PAPR reduction technique is implemented, experimental PAPR reduction gain of pilot-assisted OFDM (PA-OFDM) at a complementary cumulative distribution function (CCDF) of 10^{-3} with $P = 5$ is about 2 dB. This gain is approximately 0.2 dB less than that of analytical results. The experimental results also show that the pilot-assisted technique does not cause any significant deterioration of the bit error performance.**

***Index Terms*—optical OFDM, PAPR reduction, pilot symbol, indoor OWC, optical communications.**

I. Introduction

THE significant advantages of orthogonal frequency division multiplexing (OFDM) technology in radio frequency (RF) communications have motivated its use in optical communication systems. Such advantages include high spectral efficiency, ability to support high data rates and efficiently combat inter symbol interference (ISI) [1]. The problem of high peak-to-average power ratio (PAPR) in OFDM-based RF systems is also a major challenge in optical communication systems. However, optical wireless communication (OWC) systems differ from RF in baseband signal format, system constraints, and nonlinear characteristics of front-end devices [2]. OWC employing intensity-modulation with direct-detection (IM/DD) requires the transmit signal to be real and nonnegative in accordance with the positive nature of light intensity. The real signal is generated by imposing Hermitian symmetry (HS) on the OFDM subcarriers in frequency domain. One method of achieving nonnegativity in optical OFDM (O-OFDM) without signal clipping is the addition of sufficient direct current (DC) bias to the real-valued time domain signal. The resulting unipolar signal is then used to modulate the optical source. Hence, reducing high PAPR in O-OFDM means the optical source will operate more in its linear region, thereby reducing signal distortion.

The limited dynamic range of the optical source and the eye safety constraints further reinforce the need to reduce PAPR. In order to meet the system design requirements, O-OFDM signal with high PAPR undergo signal clipping distortion. The impact of the clipping distortion on the error performance of OFDM-based OWC system is studied in [3]. Methods used in mitigating high PAPR problem in O-OFDM include those reported in [4]–[6]. In [6], a semidefinite relaxation approach to tone injection is used to achieve PAPR reduction. Approach in [5] is based on null subcarrier shifting scheme. Authors in [4] proposed the use of pilot signal in reducing PAPR by rotating the phase of data symbols with randomly generated pilot symbol sequence. This approach is a generalised form of the widely reported selected mapping (SLM) [7] PAPR reduction technique.

The PAPR reduction capability and error performance of the pilot-assisted technique presented in [4] are based on computer simulations. In this letter, we present empirical validation and analysis of the pilot-assisted PAPR reduction technique in real indoor OWC channel following the initial principles in [4]. Experimental and theoretical results of PAPR reduction gain in PA-OFDM signal when compared with basic OFDM will be presented. Furthermore, an experimental investigation into the effect of PAPR reduction on system's error performance is also carried out.

The rest of the paper is structured as follows: description of the experimental setup is presented in Section II. Analytical evaluation of PAPR reduction of the technique is contained in Section III. In Section IV, the experimental findings, theoretical results and discussions on the performance of the technique in real OWC channel are presented. Finally, concluding remarks are given in Section V.

II. Experimental Setup

Figures 1 and 2 depict the experimental setup employed to demonstrate the performance of the pilot-assisted PAPR reduction technique in O-OFDM wireless communication system. The transmitter consists of the computer controlled vector signal generator (VSG), light emitting diode (LED) and its driver. A Thorlabs silicon amplified fixed detector is used as the optical signal receiver. The transmit and received OFDM signal are acquired with a digital storage oscilloscope.

The entire system gives a measured 3 dB bandwidth of about 17 MHz. Other parameters of the system are as listed in Table I. The electrical OFDM signal is obtained using the computer controlled VSG. Each OFDM signal frame consists of $U = 5$ data carrying symbols and a randomly generated pilot symbol, with each symbol consists of 127 subcarriers. A preamble comprising rectangular pulses is appended to the payload in time domain in order to guarantee proper

F. B. Ogunkoya, A. Shahrabi and S. Sinanović are with Glasgow Caledonian University, Glasgow, G4 0BA, UK, (email: {funmilayo.ogunkoya, A.Shahrabi, sinan.sinanovic}@gcu.ac.uk). W. O. Popoola is with The University of Edinburgh, Edinburgh, EH9 3JL, UK, (email: W.Popoola@ed.ac.uk).

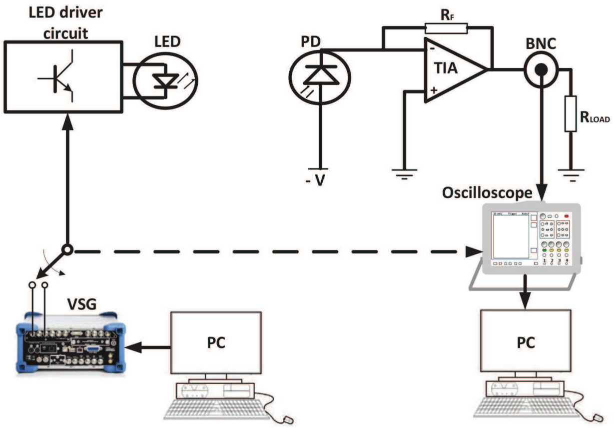

Fig. 1: An illustration of the experimental setup for the pilot-assisted PAPR reduction technique in O-OFDM communication systems.

synchronisation at the receiver as shown in the sample received signal of Fig. 3. The signal is then launched into the LED driver through the I and Q port of the VSG. Basic OFDM signal is routed via port I while PA-OFDM signal is channelled through port Q. The output of the VSG is also captured by an oscilloscope, as depicted with dashed arrow in Fig. 1, for the purpose of evaluating the PAPR of the transmitted OFDM signal. Thereafter, the signal modulates the intensity of the light source, and then radiates through an indoor OWC channel. At the receiver, the photodetector (PD) converts the intensity of the received optical signal to a proportionate electrical signal. Afterwards, the electrical signal is sampled by the oscilloscope at 50 MSamples/s, and then captured for offline processing.

The offline processing of the transmitted and received O-OFDM signal are performed using MATLAB. Once detected, the O-OFDM signal comprising the data and pilot is down-sampled to match the sampling rate of the transmitted signal. Thereafter, the PAPR of the transmit basic and PA-OFDM signal is evaluated.

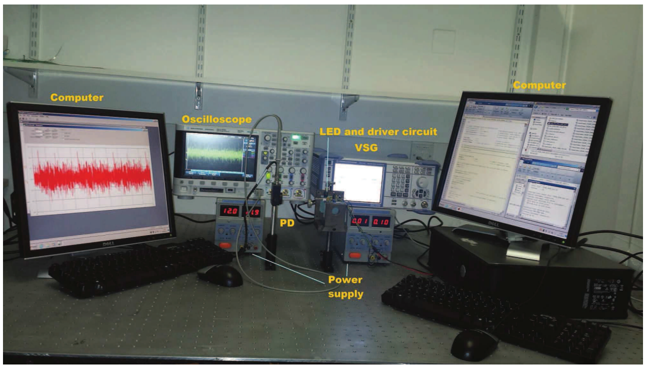

Fig. 2: Laboratory setup for the pilot-assisted PAPR reduction technique in O-OFDM communication systems.

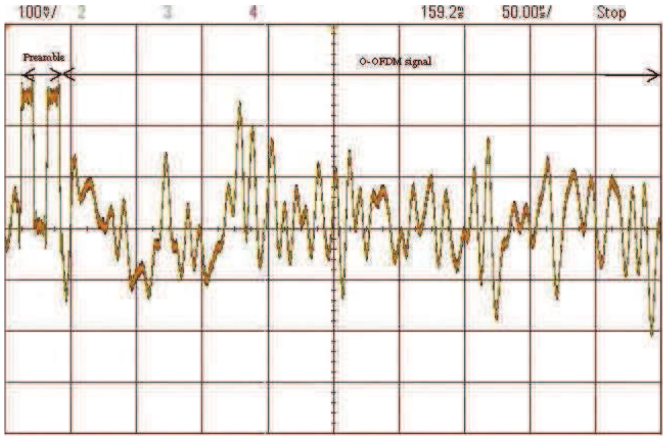

Fig. 3: A received signal showing the preamble and O-OFDM signal.

If $x(n)$ represents the detected O-OFDM signal frame oversampled L times, then the PAPR is defined as:

$$\mathrm{PAPR} \triangleq \frac{\max\limits_{0 \leq n \leq NL-1} |x(n)|^2}{E[|x(n)|^2]}, \tag{1}$$

where $E[\cdot]$ denotes the statistical expectation, $N = 2(1 + n_{\mathrm{s}})$ represents the number of subcarriers after HS operation. Likewise for bit error rate (BER) performance evaluation, the received O-OFDM signal is also synchronised and downsampled. Afterwards, the signal is converted to frequency domain followed by extraction of active data carrying signal. For channel estimation in basic OFDM, the $U = 5$ data symbols are divided by absolute value of the real part of the received pilot symbol. On the other hand, the U pilot-assisted data symbols are divided by the real part of the pilot symbol for the purpose of phase rotation reversal and channel estimation. In both cases, the received noise corrupted pilot symbol is used. Finally, M-QAM demapping operation is performed to

TABLE I: Parameters for experimental setup

Parameters	
Vector signal generator	Rohde & Schwarz (SMBV100A)
Digital storage oscilloscope	InfiniiVision DSO-X 3034A
Light emitting diode (LED)	GaAIAs IR LED (VSLY5850)
angle of half intensity $\varphi_{1/2}$	$\pm 3^{\circ}$
peak wavelength λ_p	850 nm
radiant intensity at 100 mA	600 mW/sr
Photodetector (PD)	Si PIN (PDA10A)
active area	$\varnothing$1 mm (0.8mm^2)
Peak wavelength λ_p	750 nm
Peak response $\Re(\lambda_p)$	0.45 A/W
Maximum output current I_{OUT}	100 mA
bandwidth	150 MHz
Oversampling factor (L)	4
FFT/IFFT size (NL)	1024
Active data subcarriers (n_{s})	127

obtain estimates of the transmitted data symbols. These are then compared with the transmitted data symbols for BER evaluation. The experiment is repeated for basic and PA-OFDM signal over a range of different levels of transmit power.

Electrical PAPR in O-OFDM, as given by (1), is the ratio of the maximum peak to average power of the signal. Therefore, the performance of the optical system depends on the positive and negative peak of the OFDM signal, luminous intensity and dynamic range of the optical source. If the O-OFDM signal is represented by $x(t)$, then $x_{\rm dc}$ denotes the DC voltage required to make the signal positive. Thus, the resulting unipolar signal $x_{\rm dc}(t)$ that drives the LED is proportional to $x(t) + x_{\rm dc}$. The LED converts the magnitude of the signal $x_{\rm dc}(t)$ into optical intensity. It means that the optical signal-to-noise (SNR) ratio is related to $E[x_{\rm dc}(t)]/N_o$, while the electrical SNR is $E[|x(t)|^2]/N_o$, where $E[\cdot]$ denotes the statistical expectation and N_o represents the average noise power. In this experiment, to determine the BER performance of the link, optical modulation index (OMI, β) [4] is used as the key parameter in varying the transmitted signal power level. The OMI is defined as the ratio of the maximum electrical voltage signal magnitude to LED drive voltage, that is, $\beta = |x(t)_{\max}|/x_{\rm dc}$.

III. Analytical Evaluation of PAPR Reduction in Pilot-assisted O-OFDM

In this section, we derive the closed-form expression of the PAPR distributions of PA-OFDM signal using order statistics [8] and the approximate distribution of real-valued basic OFDM signal [9]. To obtain the PAPR of a continuous time domain OFDM signal, digital-to-analogue conversion process is followed by the IFFT operation. However, the PAPR of oversampled discrete time domain signal has been established to approximate that of continuous time domain OFDM signal [10]. We obtain the distribution of PAPR with the fact that the $U+1$ symbols in the PA-OFDM frame have $U+1$ distinct maximum peaks after the IFFT operation. Using the *maximum* order statistics, we derive the cumulative distribution function (CDF) of PAPR for a single PA-OFDM frame as:

$$F_Y(y) = \Pr\left(\frac{\max\limits_{0\le n\le (U+1)(NL-1)} |x(n)|^2}{E[|x(n)|^2]} \le y\right) = \mathrm{e}^{-\frac{(U+1)Ne^{-y/2}}{\sqrt{3}}}, \tag{2}$$

where F_Y is the CDF and y is the threshold PAPR. Furthermore, the P iterations of pilot symbol sequence on a single PA-OFDM frame generate P peaks. Therefore, we use the *minimum* order statistics and (2) to analyse the PA-OFDM frame that gives the least PAPR after rotating the phase of the U data symbols with P pilots. Thus, we obtain the complementary CDF (CCDF) of PAPR of the PA-OFDM signal as:

$$\mathrm{P_{cc}(y)} = \left(1 - \mathrm{e}^{-\frac{(U+1)Ne^{-y/2}}{\sqrt{3}}}\right)^P. \tag{3}$$

IV. Results and Discussions

In this work, the pilot symbol in the PA-OFDM signal is used for reducing the transmitted signal peak as well as channel estimation. In contrast, the basic OFDM system has no PAPR reduction technique implemented. Thus, the inserted pilot symbol in the basic OFDM signal is used for channel estimation only. Also, the energy of the $M-$QAM constellation is normalized to unity. Fig. 4 represents the CCDF plot of the experimental, analytical and simulated PAPR for 16-QAM O-OFDM signal. The figure shows the PAPR of the basic and PA-OFDM signal for comparison. At a CCDF of 10^{-3} with $P = 5$, the experimental results for 6×10^3 signal frames considered show a PAPR reduction gain of approximately 2 dB. To examine the accuracy of the analysis presented in (3), result gives about 2.2 dB reduction gain at the same value of CCDF. Similarly, PAPR reduction gain via simulations also generates about 2.2 dB at CCDF of 10^{-3}. This represents a meagre 0.2 dB difference between the predicted gain via simulation/analysis and the measured. Noticeable from the plot is that this reduction gain increases as CCDF decreases in all cases.

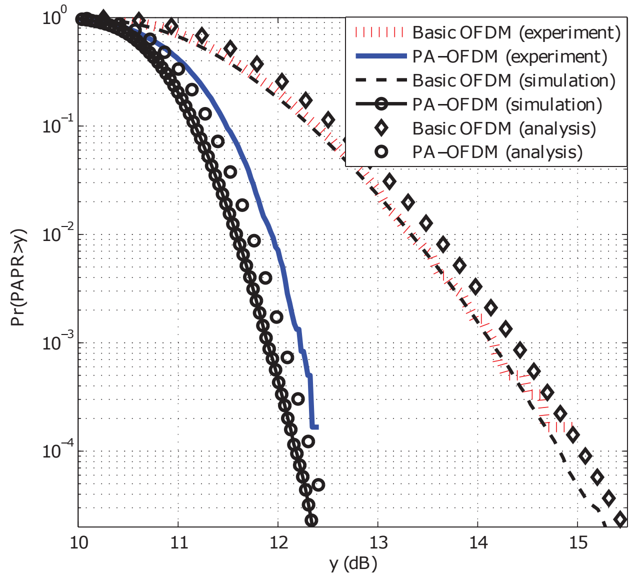

Fig. 4: CCDF plot for basic and PA-OFDM signal using 16-QAM, $L = 4$, $U = 5$, $P = 5$, $N = 256$, and equation (3).

Also shown in Fig. 5a and 5b are the distributions of experimentally measured PAPR for 16-QAM basic and PA-OFDM signal respectively with $P = 5$. PA-OFDM results indicate reduction in PAPR mean value from about 11.5 dB for basic OFDM to 10.9 dB. Moreover, the decrease in the PAPR range is a clear evidence of the PAPR reduction capability of this technique.

To investigate the effect of PAPR reduction on system's error performance, we present the BER as a function of β for both basic and PA-OFDM in Fig. 6. The figure compares

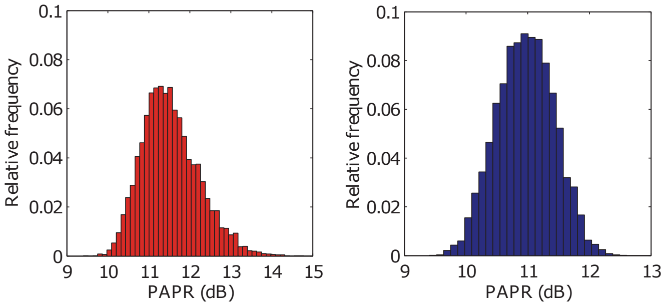

(a) Basic OFDM (b) PA-OFDM

Fig. 5: Experimental PAPR distributions for 16-QAM basic and PA-OFDM signal using $U = 5, P = 5, n_{\mathrm{s}} = 127$

the BER of basic and pilot-assisted data symbols for 4-, 16- and 64-QAM systems using $P = 5$. The comparison is important in order to experimentally investigate the tradeoff between the achieved PAPR reduction and error performance penalty of the proposed technique. There is an indication of close match between the BER performance of basic and PA-OFDM signal for 16-QAM. This agreement implies that the PAPR reduction technique does *not* degrade the error performance of the O-OFDM signal according to the system and channel conditions under investigation. Results also show similar trend of no mismatch between 64-QAM basic and PA-OFDM. For 4-QAM system, a gap of about 0.1 dB can be observed between the BER of basic and PA-OFDM. The pilot-assisted data symbols used for BER evaluation are recovered using the noisy pilot symbol. The presented results represent experimental validation of the ability of the pilot-assisted technique to reduce PAPR without introducing any additional error performance degradation.

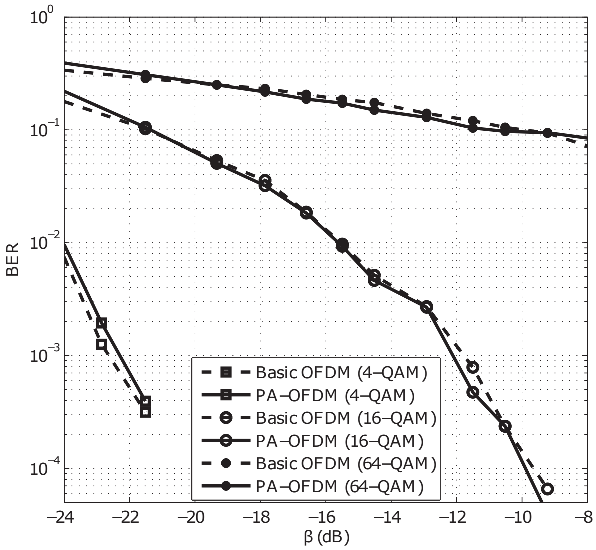

Fig. 6: Experimental BER performance for basic and PA-OFDM signal using 4-, 16- and 64-QAM, $L = 4$, $P = 5$, $U = 5$, and $n_{\mathrm{s}} = 127$.

V. Conclusion

In this letter, the PAPR reduction capability of the pilot-assisted PAPR reduction technique for O-OFDM communication systems has been validated using hardware implementation and theoretical analysis. Based on IM/DD in an indoor OWC channel, an LED is used as the optical source while a Si PIN photodiode detects the radiated O-OFDM signal. About 2 dB PAPR reduction gain is obtained from the PA-OFDM output signal of the VSG when compared with the basic OFDM at a CCDF of 10^{-3} for 16-QAM. The analytical reduction gain at the same value of CCDF is about 0.2 dB higher than that of the experiment. The experimental investigation of the effect of PAPR reduction technique on the system's error performance shows that the method does not increase the error rate. With the pilot-assisted technique, the experimental BER of 4, 16 and 64-QAM systems are identical to that of basic OFDM but their PAPR values are lower.

References

[1] Z. Ghassemlooy, W. Popoola, and S. Rajbhandari, *Optical Wireless Communications: System and Channel Modelling with MATLAB* . Boca Raton, USA: CRC Press, 2012.

[2] Z. Yu, R. J. Baxley, and G. T. Zhou, "Peak-to-Average Power Ratio and Illumination-to-Communication Efficiency Considerations in Visible Light OFDM System," in *Proc. IEEE Int. Conf. Acoust., Speech and Signal Process. (ICASSP)*, Vancouver, BC, 26–31 May 2013, pp. 5397–5401.

[3] S. Dimitrov, S. Sinanović, and H. Haas, "Clipping Noise in OFDM-Based Optical Wireless Communication Systems," *IEEE Trans. Commun.*, vol. 60, no. 4, pp. 1072–1081, Apr. 2012.

[4] W. O. Popoola, Z. Ghassemlooy, and B. G. Stewart, "Pilot-Assisted PAPR Reduction Technique for Optical OFDM Communication Systems," *J. Lightw. Technol.*, vol. 32, no. 7, pp. 1374–1382, Apr. 1, 2014.

[5] H. Chen, J. He, J. Tang, F. Li, M. Chen, and L. Chen, "Performance of 16 QAM-OFDM With New Null Subcarrier Shifting in an Intensity-Modulated Direct Detection System," *J. Opt. Commun. Netw.*, vol. 6, no. 2, pp. 159–164, Feb. 13 2014.

[6] H. Zhang, Y. Yuan, and W. Xu, "PAPR Reduction for DCO-OFDM Visible Light Communications via Semidefinite Relaxation," *IEEE Photon. Technol. Lett.*, vol. 26, no. 17, pp. 1718–1135, Sep. 2014.

[7] M. Farooqui, P. Saengudomlert, and S. Kaiser, "Average transmit power reduction in OFDM-based indoor wireless optical communications using SLM," in *Proc. 2010 Int. Conf. Elect. and Comput. Eng. (ICECE)*, Dhaka, 18-20 December, pp. 602–605.

[8] G. Casella and R. L. Berger, *Statistical Inference*, 2nd ed. Duxbury, 2002.

[9] H. Yu, M. Chen, and G. Wei, "Distribution of PAR in DMT systems," *Electron. Lett.*, vol. 39, no. 10, pp. 799–801, May 2003.

[10] K. Wong, M.-O. Pun, and H. Poor, "The Continuous-Time Peak-to-Average Power Ratio of OFDM Signals Using Complex Modulation Schemes," *IEEE Trans. Commun.*, vol. 56, no. 9, pp. 1390–1393, Sep. 2008.